20th Australian International Aerospace Congress

ISBN number: 978-1-925627-66-4

Please select category below:
Normal Paper ☒
Student Paper ☒
Young Engineer Paper ☐

Diagnostics and tracking of helicopter's engine shaft bearing inner ring degradation using cyclostationary methods

Alexandre Mauricio [1,2], Arnaud Talon [3], Vercoutter Agathe [3] , Karl Janssens [4] and Konstantinos Gryllias [1,2]

[1] *Department of Mechanical Engineering, Faculty of Engineering Science, KU Leuven, 3001, Leuven, Belgium*
[2] *Dynamics of Mechanical and Mechatronic Systems, Flanders Make, Leuven, Belgium,*
[3] *SAFRAN Helicopter EnginesAvenue Joseph Szydlowski 64511 Bordes - France*
[4] *Siemens Industry Software NV, Interleuvenlaan 68, B-3001, Leuven, Belgium*

Abstract

The components of an engine's helicopter gearbox are vulnerable to fatigue and therefore Health and Usage Monitoring Systems are intended to be developed, focusing towards early, accurate and on time detection of degradation's initialisation with limited false alarms and missed detections. The main aim of HUMs is to enhance the helicopters' engine operational reliability and functionality and to improve flight airworthiness.

Bearings are one of the components of essential interest of helicopter's engine drivetrains, as they support the rotating components or gears, and early degradation detection is necessary to prevent sudden breakdown. On the other hand, bearing signals are often masked by noise and other vibration sources, which further challenges their early detection. Over the recent decade, several cyclostationary tools have been proposed in order to extract the bearing health state information from vibration data. These methods are based on the demodulation of the signals using either the Hilbert Transform or the Spectral Correlation and/or Coherence, in tandem with band pass filtering using band selection tools.

In this paper, the performance of several cyclostationary-based indicators targeting to early bearing degradation detection is evaluated on a special dataset, including vibration and particle data, captured on a dedicated test bed of a helicopter engine drivetrain during a lifetime test. A bearing with an inner race indented in three positions was mounted on the test bed and was run until its end of life, when the full surface of the inner race was spalled.

Keywords: Condition monitoring, vibration analysis, bearing diagnostics, cyclostationarity, helicopter drivetrain

Introduction

In order to ensure safety and improve engine efficiency during operation, Research and Development programs are conducted on engine bearings especially due to their high speed and heavy load operating conditions which may cause fatigue and degradation of their rotating components. However, helicopter engines are complex rotating machinery and the vibration signatures generated due to degradation of internal components, such as bearings, are

commonly hidden beneath the noise level or masked by other rotating components' signals, making their early, accurate and on time detection rather challenging [1,2].

As diagnosis via the direct analysis of raw time domain vibration signals is rather difficult, condition monitoring of rotating structures is based on advanced signal processing techniques targeting to the extraction of the fault information. A common approach is to demodulate the signals in order to detect modulations which correspond to the characteristic fault frequencies describing the health condition of the rotating structure. Before the demodulation process, usually a band pass filter around the resonant frequencies, excited due to the fault impulses, is applied. The band can be selected either by engineering experience or by band selection tools such as the Fast Kurtogram [3].

During the last decade, specific attention has been paid to cyclostationary-based tools for condition monitoring of bearings and gears, including Cyclic Spectral Correlation (CSC) and Cyclic Spectral Coherence (CSCoh), as they are able to reveal hidden modulations on weak signals masked by noise [4,5]. The results of these methods are represented in a difficult to analyse 2D bi-variable map but the integration along one of its axes results in an equivalent demodulated spectrum, where fault identification can be easily performed. Estupinan and White [6] detected the ball spin and the cage frequencies on a CSCoh bi-variable map while analysing a degradation test of a helicopter gearbox. Even though diagnosis through the analysis of the bi-variable map requires high expertise, the method achieved high performance in detecting the characteristic ball spin frequency of defect bearings that were non-detectable using classical methods [7,8].

The objective of this paper is to evaluate the performance of the recently proposed cyclostationary-based tools, such as the CSC and CSCoh, as methods for bearing diagnostics in helicopter engines and to track the severity level of the damage over time. The performance of different demodulated spectra estimated based on the integration of the CSC and CSCoh bi-variable map in specific frequency bands are analysed and their corresponding advantages are explained. The methods are tested, validated and compared on a dedicated dataset, which includes the degradation of inner race damage of a helicopter drivetrain. The rest of the paper is organised as follows. The theory of the methods is briefly presented in the following section. Then the test setup and the dataset are detailed. Moreover the proposed methodologies are applied on the experimental dataset and the results are analysed. In the end, the paper is closing with some conclusions.

Cyclostationary tools

Rolling element bearing signals can be described as second-order cyclostationary signals, due to the slippage of elements, presenting a periodic autocorrelation of period T:

$$R_{2x}(\tau, t) = \mathbb{E}\{x(t)x(t-\tau)^*\} = R_{2x}(\tau, t+T) \quad (1)$$

where x(t) is the time signal, $\mathbb{E}$ is the ensemble average and τ is the time-lag. Cyclostationary based tools, such as Cyclic Spectral Correlation (CSC) and Coherence (CSCoh) have received an ever increasing interest due to their ability in extracting hidden modulations. CSC estimates the correlation between a modulating frequency (the cyclic frequency α) and a carrier frequency (the spectral frequency *f*) presented in a bi-variable map [10]:

$$CSC(\alpha, f) = \lim_{T\to\infty} T^{-1}\mathbb{E}[\,\mathcal{F}\big(x(t)\big)^*\mathcal{F}\big(x(t-\tau)\big)] \quad (2)$$

where F(x(t)) is the Fourier transform of the signal x(t). The Cyclic Spectral Coherence (CSCoh) is the whitened version of the CSC:

$$CSCoh(\alpha, f) = \frac{CSC(\alpha,f)}{\sqrt{CSC(0,f).CSC(0,f-\alpha)}} \quad (3)$$

The integration of the bi-variable maps over a band [F_1, F_2] of the spectral frequency *f* leads to the Improved Envelope Spectrum (IES) and to the Enhanced Envelope Spectrum (EES) (F_1=0, F_2=F_s/2, where F_s is the sampling frequency] which are equivalent to a demodulation spectrum:

$$EES(\alpha) = \frac{1}{F_2-F_1}\int_{F_1}^{F_2} | CSCoh(\alpha, f) | df \quad (4)$$

The cyclostationary-based tools CSCoh and CSC and the corresponding EES will be further used to analyse and track the bearing surface damage propagation.

Bearing test setup

The dedicated bearing setup which was used is described in Fig. 1. It contains a main rotor supported by two tested bearings, and a corps and a piston mechanism that apply axial load to the rotor. The aims of the R&D tests were: (a) to study the early beginning of bearing degradation and test different signal processing techniques targeting to early detection of this state, (b) to conduct a full degradation in order to study the phenomenology of degradation. During the tests, vibration signals were acquired from two accelerometers and the speed signal from a tachometer, which can be seen in Fig. 1. Two strain gauges were also mounted on the outer race of the tested bearings, along with two proximity probes.

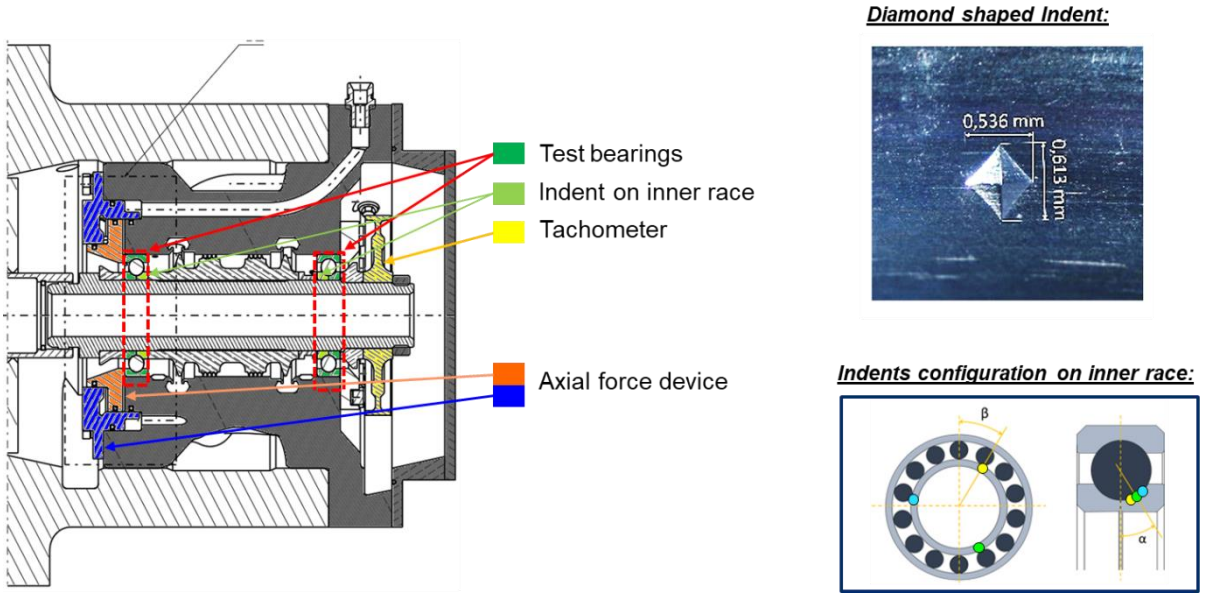

Fig. 1: Scheme of rotor with indented bearings

Three diamond shaped indents were made on the surface of the inner race separated by 120^0. The rotor rotated at a speed of 20 000 rpm for around 6 hours, until the inner race of the bearing was considered to be fully spalled reaching its end of life. Metal particle analysis of the oil was also conducted during the full duration of the test. In order to follow the degradation, the bearing was unmounted for inspection at different states and the test was stopped when the angular

propagation reached at 270°, without having a specific objective in terms of the total amount of metallic particules.

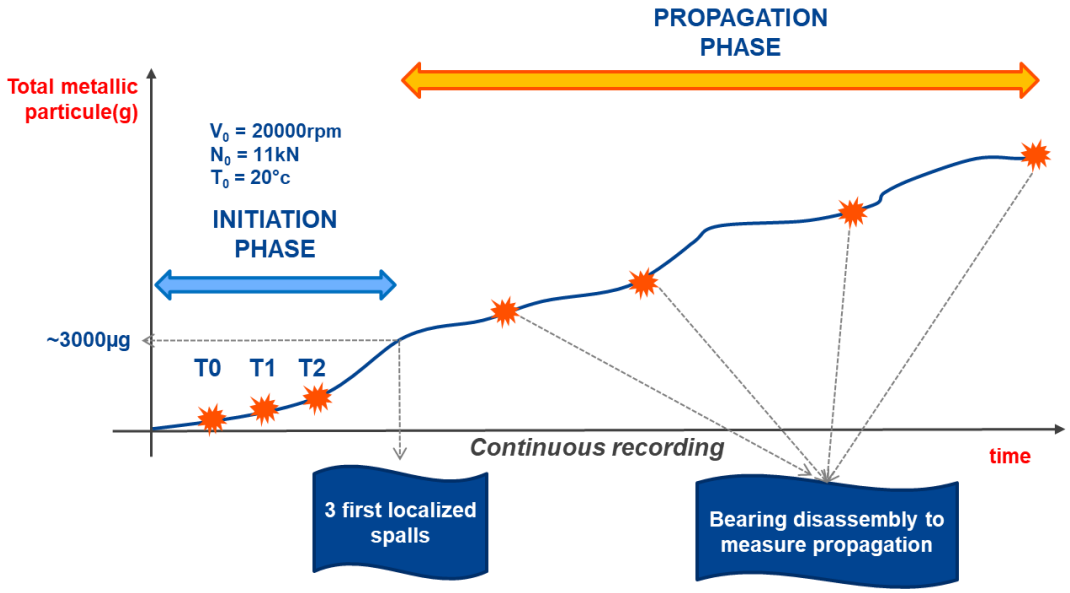

Fig. 2: Description of the initiation phase with 3 acquired signals (T0, T1 and T2), and the propagation phase with 4 signals

The tests can be separated in two phases. The first phase is considered as the initiation phase, where the small indents grow to localized spalls in the surface of the inner race. Three signals were acquired during the initiation phase:

- T0 – acquired before the detection of metal particles in the oil
- T1 – acquired after the 1st detection of metal particles in the oil
- T2 – acquired after an second increase in detection of metal particles in the oil.

The setup was dismantled at the end of the initiation phase, and localized spalling was visually confirmed on the inner race of the bearing.

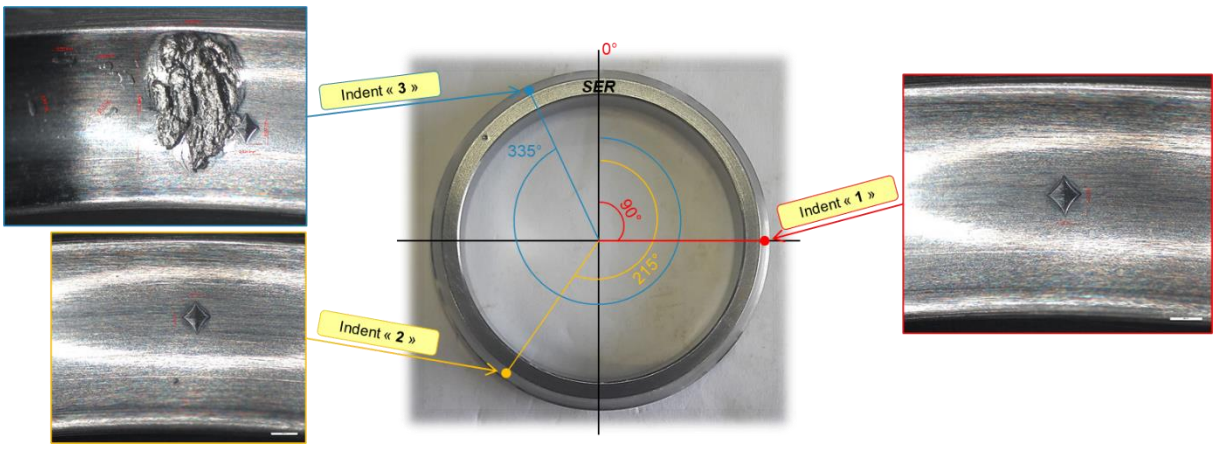

Fig. 2: Photos of the indents and the spall generation

The next phase can be described as the propagation phase, where the localized spalling propagated until the full circumference of the inner race surface was spalled. Four signals were acquired during the propagation phase and the bearing was dismounted once at mid phase, and a second time again at the end of the phase.

The sensor signals were acquired at a sampling frequency of 204.8 kHz, and the shaft speed and nominal bearing characteristic frequencies are detailed in Table 1.

Table. 1: Nominal characteristic frequencies

Characteristic Frequency	Frequency (Hz)
Speed	**335**
BPFI	**2714**
BPFO	**1977**
FTF	**134**
BSF	**1876**

Results and discussion

The signals captured from the accelerometer located near the tested bearing show a clear increase of the vibration magnitude. The first 3 signals of the initiation phase (T0, T1 and T2) show an increase of the vibration magnitude, as can be seen in Fig. 3. One signal of the propagation phase is also shown in Fig. 3, and it can be seen that the amplitude of the vibration increases and saturates at the maximum range limit of the accelerometer.

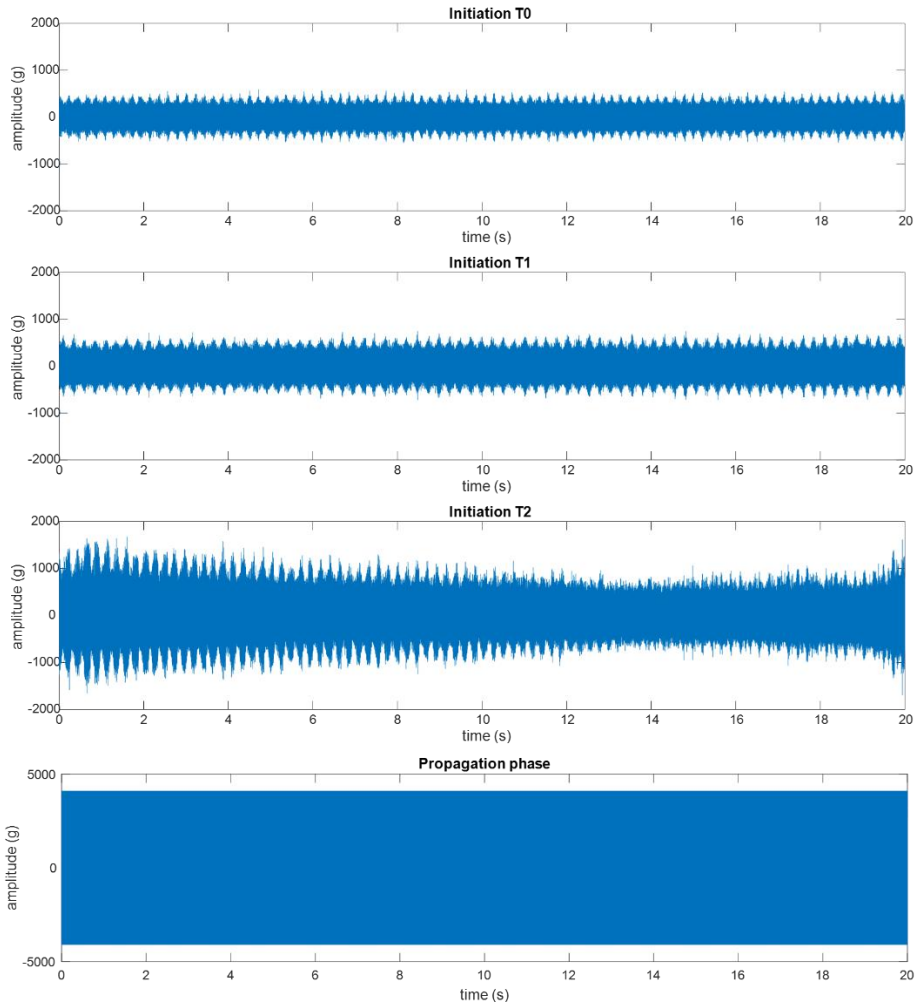

Fig. 3: Three initiation phase signals (T0, T1 and T2) and one propagation phase signal

Analysis of the CSC map of the T0 signal barely exhibits the first BPFI at low amplitude near the background level, and exhibits a main resonance carrier frequency of 52 kHz, as can be seen in Fig. 4.

For the following signals, T1 and T2, the amplitude of the BPFI harmonics is seen to increase in the same carrier of 52 kHz. Extraction of the EES from the CSC results in a consequent increase of the BPFI harmonics and the shaft frequency amplitudes, that modulate the BPFI, as time progresses and the indent progresses from indent to a localized spall. The CSC maps and the resulting EES for the initiation phase signals can be seen in Fig. 4.

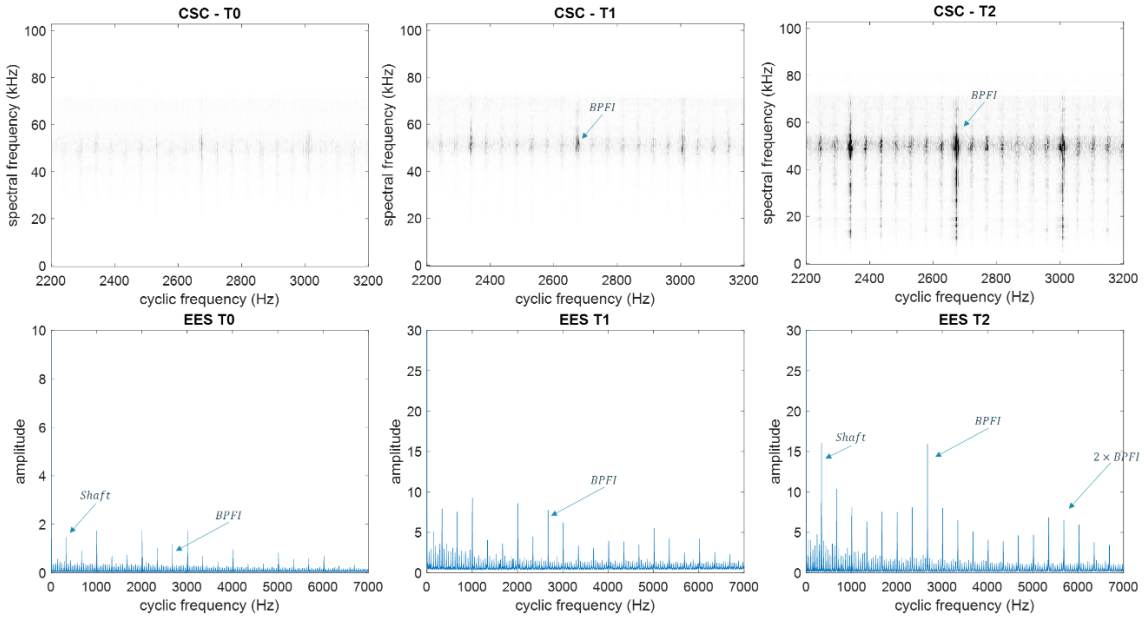

Fig. 4: Cyclic Spectral Correlation (first raw) and the corresponding Enhanced Envelop Spectrum (second raw) of the 3 signals at the initiation phase: (left) T0, (middle) T1, (right) T2

Analysis of the CSCoh shows similar results, with a small amplitude of the BPFI harmonics at the first T0 signal, and an increasing participation of the BPFI harmonics in the map in T1 and T2 signals, as can be seen in Fig. 5.

The carrier frequency of the BPFI is also seen to spread from a narrower band to a wider band from T1 to T2 signals. The extraction of the EES of the signals results in increasing amplitudes of the BPFI harmonics from T0 to T2.

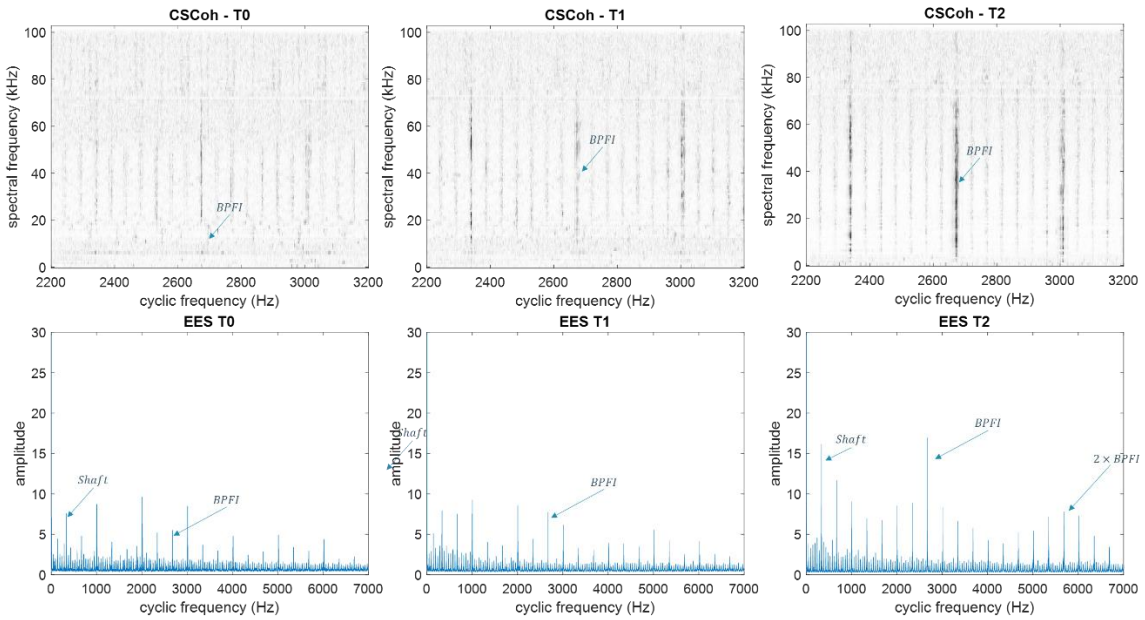

Fig. 5: Cyclic Spectral Coherence (first raw) and the corresponding Enhanced Envelope Spectrum (second raw) of the 3 signals at the initiation phase: (left) T0, (middle) T1, (right) T2

The vibration signals captured during the propagation phase demonstrate a dominant BPFI related signature. As such, both the CSC and CSCoh show clear harmonics of the shaft speed and the BPFI at high amplitudes. The 8th harmonic of the shaft speed is close to the 1st harmonic of the BPFI, and both can be detected as separated frequencies in the EES, as is shown in Fig. 6, where the harmonics of the shaft speed and the sidebands around the BPFI are clearly identified.

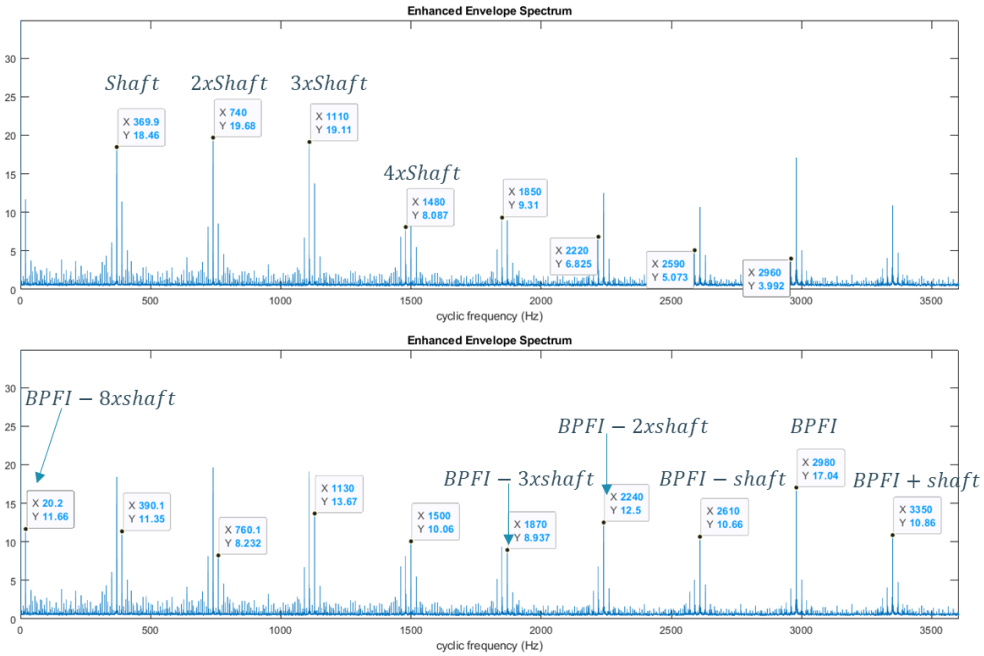

Fig. 6: Enhanced Envelope Spectrum of propagation phase: (top) shaft speed harmonics; (bottom) BPFI and its sidebands at the shaft speed frequency

The amplitude of the harmonics of the characteristic frequencies related to the damage, in other words the BPFI and the shaft speed, are tracked as indicators for health estimation from the EES based on the CSC and CSCoh. A square moving window of 1 second with 50% overlap is applied on the signals as function of time. Each windowed signal results in one EES and from each signal the indicators are extracted. This results in a total of 262 signals, from which the first 66 signals correspond to the initiation phase, and the following 196 signals correspond to the propagation phase.

The amplitudes at the shaft speed and at the BPFI on the EES based on the CSC are tracked and shown in Fig. 7. It can be seen that both indicators increase with time during the initiation phase, where the indent on the inner race evolves to a localized spall. Following to the propagation phase, the indicators are seen to be stable with no upward trending, as the localized spall has already propagated to a distributed spall covering fully the inner race surface.

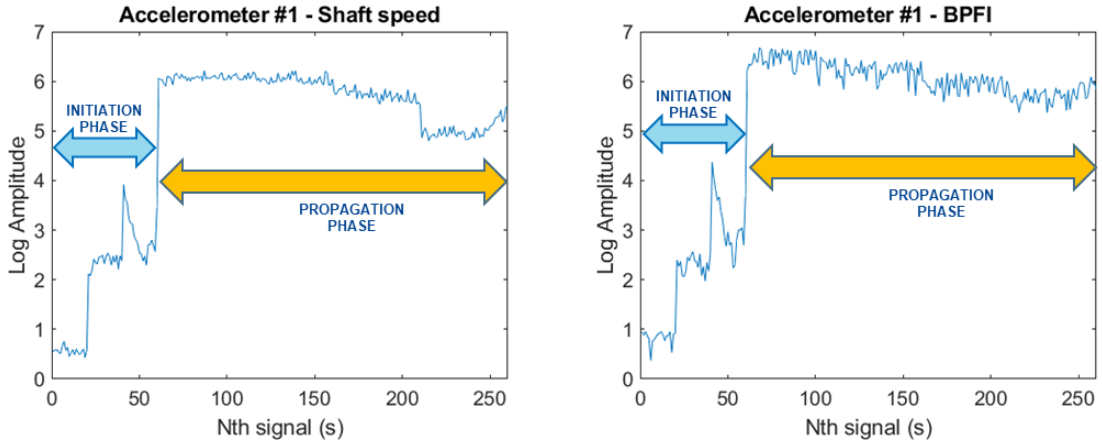

Fig. 7: Amplitude tracking of the shaft speed and BPFI as a feature on the Spectral Correlation

The amplitudes at the shaft speed and at the BPFI on the EES based on the CSCoh is tracked and shown in Fig. 8. The indicators also show an upward trend during the initiation phase, followed by stable levels throughout the propagation phase. The CSCoh based indicators appear to be more noisy when compared to the CSC based indicators of Fig. 7. This is due to the normalization procedure of the CSCoh, which is followed before the estimation of each EES. As a result the CSCoh indicators provide a clearer detection of the hidden cyclostationary modulations compared to the CSC indicators, but on the other hand they are less effective in defect tracking and trending.

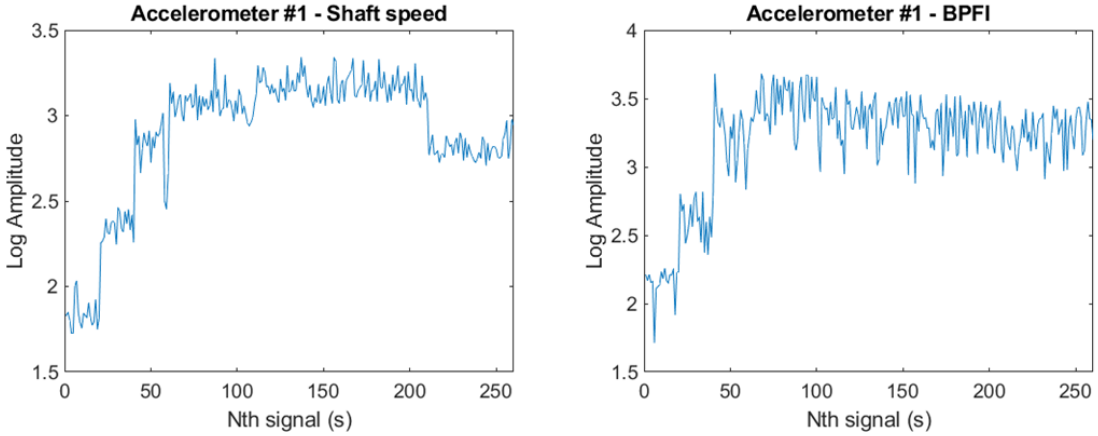

Fig. 8: Amplitude tracking of the shaft speed and BPFI as a feature on the Spectral Coherence

Conclusion

In this paper cyclostationary tools have been applied to acceleration signals captured during a degradation of inner race damage of a helicopter's engine bearing. Along with the vibration signals, metal particle analysis was performed to track the severity level of the degradation. The EES based on the CSC and CSCoh have been analysed and detected successfully the degradation related characteristic frequencies, such as the shaft speed and the BPFI. Tracking of these amplitudes show an increasing trend which follows the increasing degradation during the initiation phase, as the degradation evolves from small indent to localized spalling. During the following propagation phase, where the distributed spall further propagates, the indicators remain stable at high values. Moreover the CSC-based indicators show a higher performance in tracking and trending the damage severity, as they does not contain the normalizing procedure of the CSCoh.

References

1. Zhou, L., and Duan, F., and Corsar, M., and Elasha, F., and Mba, D., 2017. "A study on helicopter main gearbox planetary bearing fault diagnosis". *Applied Acoustics*. (2017).

2. Elasha, F., Greaves, M., and Mba, D., "Bearing signal separation of commercial helicopter main gearbox". *Procedia CIRP*, 59, pp. 111 – 115. (2017)

3. Antoni, J., "Fast computation of the kurtogram for the detection of transient faults". *Mechanical Systems and Signal Processing*, 21, pp. 108 – 124 (2007).

4. Antoni, J., "Cyclic spectral analysis in practice". *Mechanical Systems and Signal Processing*, 21 (2), pp. 597– 630. (2007).

5. Antoni, J., Abboud, D., and Xin, G., "Cyclostationarity in condition monitoring: 10 years after", *Proceedings of ISMA 2016 including USD,* 19- 21 Sep. (2016).

6. Estupinan, E. and White, P., "Cyclostationary Analysis As A Tool For The Detection Of Incipient Faults In Helicopter Gearboxes", *Proceedings of the 2nd World Congress on Engineering Asset Management (EAM) and The 4th International Conference on Condition Monitoring*, 11 - 14 Jun pp. 607-614. (2007),

7. McInerny, S.A. and Hardman B., and Sun Q., "Investigation of fault detection algorithms applied to a helicopter input pinion bearing". *Technical Report.* (2004).

8. Dawson, F.G., and Killian, K.V., "Alternate Source Endurance Qualification Test of UH-60 Black Hawk Transmission, Test Report," NAWCAD, Patuxent River, MD, June (2001).

9. Randall R.B. and Antoni J., "Rolling element bearing diagnostics—A tutorial" *Mechanical Systems and Signal Processing*, 25 pp. 485-520 (2011),

10. Randall R.B. and Antoni J., and Chobsaard, J., 2001. "The relationship between spectral correlation and envelope analysis in the diagnostics of bearing faults and other cyclostationary machine signals". *Mechanical Systems and Signal Processing*, 15 pp. 945 – 962, (2011)